SHEP-12-35

The 125 GeV Higgs signal at the LHC in the CP Violating MSSM

Amit Chakraborty[a], Biswaranjan Das[b], J. Lorenzo Diaz-Cruz[c], Dilip Kumar Ghosh[a], Stefano Moretti[d] and P. Poulose[b]

[a] *Department of Theoretical Physics, Indian Association for the Cultivation of Science, 2A & 2B, Raja S.C. Mullick Road, Jadavpur, Kolkata 700 032, India.*

[b] *Department of Physics, IIT Guwahati,Assam 781039, India.*

[c] *Facultad de Ciencias Físico-Matemáticas, Benemérita Universidad Autónoma de Puebla, Puebla, México*

[d] *School of Physics & Astronomy, University of Southampton, Highfield, Southampton SO17 1BJ, UK.*

Abstract

The ATLAS and CMS collaborations have observed independently a new Higgs-like particle with a mass $M_h \sim 125$ GeV. It is of great interest nowadays to understand the origin and identity of such a particle, whether it comes from the Standard Model (SM) or from some extension of it, such as Supersymmetry (SUSY). The simplest SUSY extension of the SM, the so-called Minimal Supersymmetric Standard Model (MSSM), predicts the tree-level mass relation $M_h \leq M_Z$, so that significant radiative corrections, coming from heavy stop masses and/or large values of $\tan\beta$, are required in order to reach a 125 GeV Higgs boson mass, as well known. Literature already exists within the MSSM also for the case of attempting to explain other ATLAS and CMS results, in particular, an apparent excess in the gg-induced $\gamma\gamma$ channel, over and above the SM predictions in presence of a Higgs boson. Here, we are interested in evaluating the modifications on these (CP-conserving) MSSM results that appear within the CP-violating version of the MSSM. Namely, we will evaluate the role of the complex phases of the soft SUSY terms and the μ parameter on both the mass of the light Higgs boson, h_1, and their effects on the rates for the process $gg \to h_1 \to \gamma\gamma$.

E-mail: tpac@iacs.res.in, biswaranjan@iitg.ernet.in, jldiaz@fcfm.buap.mx, tpdkg@iacs.res.in, S.Moretti@soton.ac.uk, poulose@iitg.ernet.in

1 Introduction

The experimental observation of the Standard Model (SM) Higgs boson and the determination of its properties were the main motivations behind the construction of the Large Hadron Collider (LHC). Very recently, both the ATLAS and CMS experiments have reported the hint of a Higgs-like particle having mass around 125 GeV [1,2]. It is almost evident from the results that the observed signals in the different production and decay channels seem to follow the SM predictions. However, perhaps due to the presence of large experimental uncertainties, there are some deviations in some of the individual channels from the SM expectations. But, it is also possible that such deviations could signal the presence of physics Beyond the SM (BSM). For instance, one can explain these results in models with an extended Higgs sector like those embedded in Supersymmetry (SUSY) [3–6].

SUSY is one of the most popular extensions of the SM, with motivations that include: i) the solution of the hierarchy and naturalness problems of the SM; ii) the unification of the SM gauge couplings at some high scale close to the Planck mass; iii) the provision of a Dark Matter (DM) candidate (so long that R-parity conservation is postulated); iv) being a natural ingredient of String theories.

The Minimal Supersymmetric Standard Model (MSSM) though, the simplest realization of SUSY, predicts the maximum tree-level value of the Higgs mass to be $M_h \leq M_Z$. However, only mild radiative corrections are needed in order to push M_h to be above the latest LEW bound, $M_h > 114$ GeV. However, making the Higgs mass to reach around 125 GeV requires the inclusion of sizable top/stop loop corrections, which depends quadratically on the top quark mass and logarithmically on the stop masses, combined with a large value of $\tan\beta$, the ratio of the Vacuum Expectation Values (VEVs) of the two Higgs doublets pertaining to the MSSM. Several studies have already been performed in the context of different SUSY models, including the MSSM [7] (also the constrained version [8]), NMSSM [9], (B-L)SSM [10]. All of them have predicted a SM-like Higgs boson with mass around 125 GeV and found solutions explaining the excess in the di-photon channel.

Another route to follow in order to obtain similar results is to consider the possibility of having CP-violating phases in (some of) the SUSY parameters that can substantially modify Higgs boson phenomenology at colliders at both mass spectrum and production/decay level [11, 12]. In this paper, we will indeed study the prospect of having a Higgs boson in the context of such a scenario with a mass around 125 GeV and event rates compatible with all LHC data, not only those used in the Higgs boson search but also those exploited in various SUSY studies.

Things go as follows. The Higgs potential of the MSSM is CP invariant at tree level. Several studies have been performed to break the CP invariance of the Higgs potential spontaneously [13]. However, these possibilities are now almost ruled out by the experiments [14]. Instead, CP violation can be induced explicitly in the Higgs sector of the MSSM. This can be achieved by introducing the

complex parameters that break CP invariance in the sfermion and chargino/neutralino sectors of the MSSM. There are many new parameters which could in principle be complex and thus possess CP-violating phases, like the Higgsino mass parameter (μ), the soft SUSY breaking gaugino masses (M_1, M_2, M_3) and the soft trilinear couplings A_f of the Higgs boson to the (massive) sfermions of flavour f. In general, each of these phases can be independent. CP violation effects are then carried into the Higgs sector through the interactions of the two Higgs doublets with the sfermions and/or charginos/neutralinos.

In short, in this study, we will study the possibility to have Higgs signals with mass around 125 GeV in the context of such a CP-violating MSSM (CPV-MSSM), which are in agreement with the aforementioned LHC data as well as other experimental constraints. We shall look for parameters of the model for which there exists agreement for both the Higgs mass and also with the rate of the most anomalous signal $gg \to h \to \gamma\gamma$, while not falling foul of the limits existing in all the other production and decay channels currently tested by the experiments. We shall also investigate the dependence of the feasible CPV-MSSM signals on the couplings of the Higgs boson to both the relevant particle and sparticle states entering the model spectrum, as well as upon the masses of the latter, thereby aiming at a general understanding of the role of the complex phases.

The paper is structured as follows. In the next section we give a brief introduction to the Higgs sector of the CPV-MSSM. In Sect. 3 we investigate the possible numerical values of its parameters after performing a scan of the CPV-MSSM parameter space against available experimental constraints. In Sect. 4 we present our results on Higgs production and decay processes in connection with the LHC Higgs data. Finally, we conclude in Sect. 5.

2 A light Higgs mass within the CPV-MSSM

Within the theoretical framework of the MSSM, non-zero phases of μ, M_i(i= 1,2,3) and/or A_f can induce CP violation in the Higgs sector radiatively, via the interactions of the Higgs bosons with the sfermions and gauginos. Thus these complex phases will break the CP invariance of the tree level scalar potential. As a result there will appear modifications to the values of the Higgs masses as well as the Higgs couplings. These effects could be described either diagrammatically or through the effective potential technique. Either way, we only need to recall here the basics. The starting point is the two Higgs doublets of the MSSM, which can be written as gauge eigenstates in the form

$$\Phi_1 = \begin{pmatrix} \phi_1^+ \\ \phi_1^0 + i\eta_1^0 \end{pmatrix}, \qquad \Phi_2 = \begin{pmatrix} \phi_2^0 + i\eta_2^0 \\ \phi_2^- \end{pmatrix}, \tag{1}$$

with

$$< \Phi_1^0 >= \frac{1}{\sqrt{2}} \begin{pmatrix} 0 \\ v_u \end{pmatrix}, \qquad < \Phi_2^0 >= \frac{1}{\sqrt{2}} \begin{pmatrix} v_d \\ 0 \end{pmatrix}$$

and where η_i^0 (i = 1,2) are the pseudoscalar components of the two Higgs doublets.

In the presence of CP-violating phases in the scalar potential the mass matrix for the neutral Higgs bosons assumes the general form

$$\mathcal{L}_{\rm mass} = \left(\begin{array}{cc|cc} \eta_1^0 & \eta_2^0 & \phi_1^0 & \phi_2^0 \end{array} \right) \left(\begin{array}{c|c} \mathcal{M}_P^2 & \mathcal{M}_{SP}^2 \\ \hline \left[\mathcal{M}_{SP}^2\right]^T & \mathcal{M}_S^2 \end{array} \right) \left(\begin{array}{c} \eta_1^0 \\ \eta_2^0 \\ \hline \phi_1^0 \\ \phi_2^0 \end{array} \right). \tag{2}$$

This 4×4 mass matrix is divided into 2×2 blocks with $\mathcal{M}_P^2$, $\mathcal{M}_S^2$ and $\mathcal{M}_{SP}^2$ as the independent components where the last quantity is absent in the CP-conserving MSSM (CPC-MSSM). This term is generated in the CPV-MSSM through one-loop corrections [15]. Different contributions to the terms in the 2×2 matrix $\mathcal{M}_{SP}^2$ can be summarized as follows [16]:

$$\mathcal{M}_{\rm SP}^2 \approx \mathcal{O}\left(\frac{M_t^4 \mid \mu \mid\mid A_t \mid}{v^2 32\pi^2 M_{\rm SUSY}^2}\right) \sin\Phi_{\rm CP} \times \left[6, \frac{\mid A_t \mid^2}{M_{\rm SUSY}^2}, \frac{\mid \mu \mid^2}{\tan\beta M_{\rm SUSY}^2}, \frac{\sin 2\Phi_{\rm CP} \mid A_t \mid\mid \mu \mid}{\sin\Phi_{\rm CP} M_{\rm SUSY}^2}\right], \tag{3}$$

where $\Phi_{\rm CP} = {\rm Arg}(A_t\mu)$, $v = 246$ GeV and the mass scale $M_{\rm SUSY}$ is defined by

$$M_{\rm SUSY}^2 = \frac{m_{\tilde{t}_1}^2 + m_{\tilde{t}_2}^2}{2}\,, \tag{4}$$

with $m_{\tilde{t}_1}$ and $m_{\tilde{t}_2}$ being the stop masses.

One can easily estimate the degree of CP violation in the Higgs sector by considering the dominant one(s) of these contributions. For example, sizeable scalar-pseudoscalar mixing is possible for a large CP-violating phase $\Phi_{\rm CP}$, $|\mu|$ and $|A_t| > M_{\rm SUSY}$. Apart from a massless Goldstone boson G^0, which does not mix further with the other neutral states, the 4×4 mass matrix effectively reduces to a 3×3 Higgs mass-squared matrix $\mathcal{M}^2$, in the basis (A, ϕ_1^0, ϕ_2^0), where A is the appropriate eigenstate of $\mathcal{M}_P^2$. The 3×3 symmetric matrix $\mathcal{M}_{ij}^2$ can be obtained by an orthogonal matrix $\mathcal{O}$, i.e., $M_i^2\delta_{ij} = O_{ik}\mathcal{M}_{kl}^2 O_{jl}$.

The physical mass eigenstates h_1, h_2 and h_3 (in ascending order of mass) are actually mixtures of the CP-odd A and the CP-even ϕ_1^0 and ϕ_2^0, i.e., states of indefinite CP. Moreover, as A is no longer a physical state, the charged Higgs boson mass $M_{H^\pm}$ is a more appropriate parameter for the description of the CPV-MSSM Higgs sector in place of M_A often used in the CPC-MSSM.

3 CPV Higgs mass and the available parameter space

As explained, the non-trivial CPV phases modify the Higgs mass significantly by introducing mixing between the scalar and pseudo-scalar Higgs sector. CPV phases can also affect the Higgs couplings

with the gauge bosons and fermions, altering significantly their tree level values. For example, in a situation with maximal CP violation, known as CPX scenario, one can have the lightest Higgs boson which is almost CP-odd with a highly suppressed coupling to a pair of Z's [17].

In order to study the mass and couplings of the Higgs bosons of the CPV-MSSM, we need to consider the relevant parameter space. However, the latter contains a large number of arbitrary free parameters due to an extended and more complex theoretical framework than that of CPC-MSSM. We have used CPsuperH (version 2.3) [18] to define and scan the CPV-MSSM parameter space (randomly). The ranges of variation of the input parameters are:

1. For the parameters defining the Higgs sector at tree level:

   $1 < \tan\beta < 20, \quad 100 \text{ GeV} < M_{H^\pm} < 300 \text{ GeV}.$

2. For first two gaugino masses:

   $50 \text{ GeV} < M_1 < 500 \text{ GeV}, \qquad 100 \text{ GeV} < M_2 < 2000 \text{ GeV}.$

3. For the 3rd family sfermion masses:

   $500 \text{ GeV} < (M_{Q3},\ M_{U3},\ M_{D3},\ M_{L3},\ M_{E3}) < 2000 \text{ GeV},$

4. For the 3rd family trilinear scalar couplings and μ-parameter:

   $500 \text{ GeV} < (A_t,\ A_b,\ A_\tau,\ \mu) < 2000 \text{ GeV}.$

5. For the phases appearing in the above parameters:

   $\phi_{A_t} = \phi_{A_b} = \phi_{A_\tau} = \phi_3 = 0^o, 90^o.$

6. For the phase of the gaugino mass parameter M_3:

   $\phi_3 = 0^o, 90^o.$

While the following parameters are fixed during the scan:

1. Gaugino mass parameter:

   $M_3 = 1200 \text{ GeV}$

2. Trilinear coupling of 1st and 2nd sfermion families:

   $|A_e| = |A_\mu| = |A_u| = |A_d| = |A_c| = |A_s| = 0.$

3. Phases of the trilinear couplings for the first two generations:

   $\phi_{A_e} = \phi_{A_\mu} = \phi_{A_u} = \phi_{A_d} = \phi_{A_c} = \phi_{A_s} = 0.$

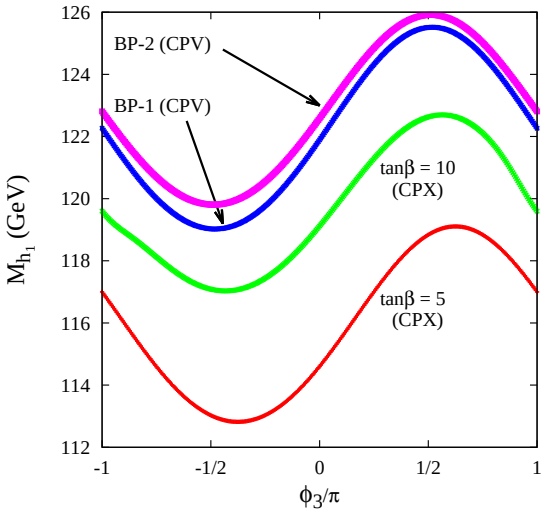

Figure 1: The dependence of the lightest Higgs boson mass, M_{h_1}, in the CPV-MSSM as a function of the CPV phases following our scans (upper two curves) against two benchmark points in the CPX scenario, for two different values of $\tan\beta$ (lower two curves), as detailed in the text.

4. Phase of the μ term and gaugino mass parameters M_1 & M_2:

   $\phi_\mu = \phi_1 = \phi_2 = 0$.

5. A hierarchy factor between first two and 3rd generations soft masses of 20.

We have performed a fully randomized scan of 5×10^5 points over the aforementioned ranges of the parameters while the two phases $\phi_{A_f}, (f = t, b, \tau)$, and ϕ_3 are kept fixed at 90^o. While imposing the different collider constraints on the parameter scan, we primarily demand that the lightest Higgs boson mass (M_{h_1}) should always lie in the range $124 - 126$ GeV. We then impose the following constraints to select the final set of allowed parameter points for our further analysis:

- The existing LEP constraints as implemented in CPSuperH (version 2.3) [18].
- $1.1 \times 10^{-9} < \mathrm{BR}(B_s \to \mu^+\mu^-) < 6.4 \times 10^{-9}$; the recent LHCb data [19].

In the CPV case (i.e., when the common phase is set to 90 degree, the maximal CP-violating scenario) 10975 points survive the first constraint. After the implementation of the second limit we are left with only 974 points. To obtain a correspondence with the CPC-MSSM, we have proceeded

BP	M_1	M_2	M_3	$\tan\beta$	$M(H^{\pm})$	MQ3	A_t	μ	$M(h_1^0)$
1	284.3	956.3	1200	8.9	298.8	641.7	1725.9	858.3	125.5
2	291.9	550.4	1200	10.4	291.9	1176.7	1939.7	718.5	125.9

Table 1: Two benchmark points in the CPV-MSSM scenario obtained after performing a random scan over the CPV parameter space using CPsuperH (version 2.3). In addition to the values of some of the parameters, we have also presented the mass of the lightest neutral Higgs Boson h_1. We have fixed the CP-violating phases to 90^o. All masses, A_t and μ are expressed in units of GeV.

in the same way apart from setting the phases to zero, while keeping all other inputs same as the CPV ones.

In Fig.1 we display the variation of the lightest Higgs boson mass (M_{h_1}) as a function of the phase ϕ_3, while keeping $\phi_{A_f} = 90^o$. The upper two curves represent two characteristic benchmark points (BP-1 & BP-2) obtained from the scan of the CPV-MSSM parameter space, whereas the lower two curves represent the CPX scenario [16].

In Tab. 1, we have given the details of these two benchmark points, BP-1 and BP-2, where the last column gives the mass of the lightest neutral Higgs boson. These two points are illustrative of the fact that it is always possible to have the lightest Higgs boson mass around 125 GeV when one includes the sizeable corrections coming from the CPV phases onto the MSSM.

Before proceeding to analyze some LHC observables, it is important to take a look at the CPV-MSSM parameters and the particle spectrum after some selection is enforced upon the points obtained in the random scan. In Fig. 2(a) and (b) we have showed the allowed parameter space in the $\tan\beta - M_{H^{\pm}}$ and $A_t - A_b$ planes, respectively. The red/medium-grey points denote the region of the parameter space which satisfies LEP constraints, including the limit on the lightest Higgs boson mass (as mentioned before). From Fig. 2(a) one can conclude that the current limit on BR($B_s \to \mu^+\mu^-$) prefers low to medium values of $\tan\beta \sim 7 - 14$ and a somewhat heavier charged Higgs mass $M_{H^{\pm}} \gtrsim 200$ GeV (green/light-grey points). In the CPC-MSSM, the BR($B_s \to \mu^+\mu^-$) $\propto \tan\beta^6/M_A^4$, where M_A is the pseudo-scalar Higgs boson mass, normally used to define the Higgs sector of the CPC-MSSM. However, in the CPV-MSSM, due to CP mixing, we do not have an exact CP eigenstate for the physical neutral Higgs bosons so that the charged Higgs mass ($M_{H^{\pm}}$) plays the role of M_A here and controls the Higgs sector. Hence, to satisfy the current limit on the BR($B_s \to \mu^+\mu^-$), one requires a heavier neutral Higgs mass (this automatically implies a heavier $M_{H^{\pm}}$) and a lower $\tan\beta$. In this analysis, our main motivation is to find out the range of the CPV-MSSM parameters where one can have an enhanced $h_1 \to \gamma\gamma$ rate with respect to the SM prediction. Once we impose this, the final allowed parameter points shrink to the region depicted by the blue/dark-grey dots. Let us now turn our attention to the Fig. 2(b), which clearly shows that, in order to have a lightest Higgs boson mass within $124 - 126$ GeV, a heavy A_t is preferred.

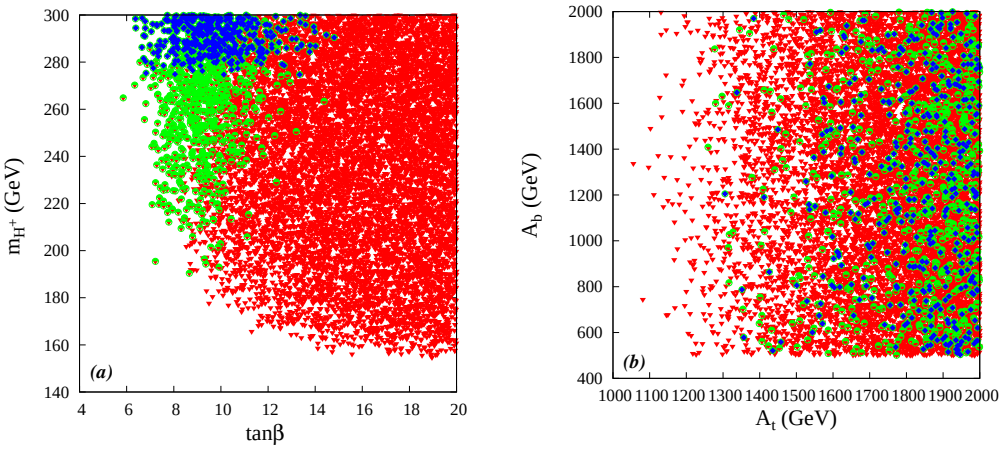

Figure 2: Constraints on the (a) $\tan\beta - M_{H^\pm}$ plane and (b) A_t - A_b plane obtained after scanning the CPV parameter space randomly. The red (medium grey), green (light grey) and blue (dark grey) points are allowed by the LEP constraints with 124 GeV $< M_{h_1} <$ 126 GeV, BR($B_s \to \mu^+\mu^-$) limit and $R_{\gamma\gamma} > 1$ (see eq. (6)), respectively.

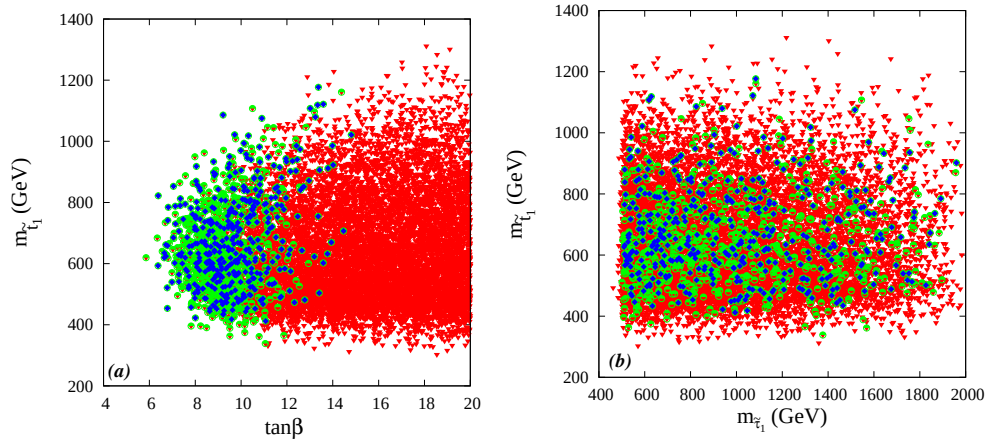

Figure 3: Constraints on $\tan\beta - m_{\tilde{t}_1}$ plane (a) and $m_{\tilde{t}_1} - m_{\tilde{\tau}_1}$ plane (b). The constraints applied and color/grey codes are same as in Fig.2.

This can be understood from the fact that large A_t corresponds to large mixing in the stop sector which in turn keeps the lightest Higgs boson mass light. It is also very clear that large values of A_t are preferred for the sought enhancement in the di-photon channel while there is no such a strong dependence on A_b.

Fig. 3 summarizes the particle spectrum in the context of the CPV-MSSM under the same conditions as previously explained, maintaining the same colour coding. It shows in particular

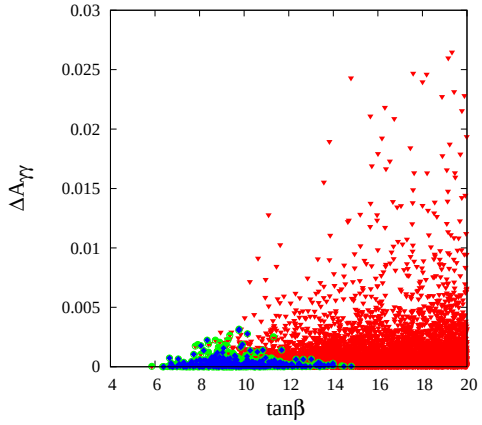

Figure 4: Scatter plots in $\tan\beta - \Delta A_{\gamma\gamma}$ plane. The constraints applied and color /grey codes are same as in Fig.2.

that lightest stop mass, $m_{\tilde{t}_1}$, can be as low as 400 GeV, see Fig. 3(a,b). We have also analyzed the possibility to observe an enhanced di-photon rate due to the presence of light staus. The contribution coming from the staus are primarily controlled by μ and tanβ and, ignoring subleading terms, one can approximate their contribution to the total amplitude of the $h_1 \to \gamma\gamma$ process by the quantity $\Delta A_{\gamma\gamma}$ which can be written as [20]:

$$\Delta A_{\gamma\gamma} \propto -\frac{2(\mu \tan\beta)^2 m_\tau^2}{3\left[M_{L3}^2 M_{E3}^2 - M_\tau^2(\mu\tan\beta)^2\right]}. \tag{5}$$

As we know, in the SM, the di-photon amplitude of the top-quark and W-boson loop comes with opposite sign and the latter is dominant. Hence, to get an enhancement of the partial $\gamma\gamma$ width, any new contribution should constructively interfere with the W-boson contribution. To achieve this, in Ref. [20], it has been shown that, in the CPC-MSSM, the additional contribution from the stau loops should be of order one and must interfere constructively with the dominant W-boson contribution. It is very clear that to have such a $\mathcal{O}(1)$ contribution one must have large $\mu\tan\beta$. In our analysis though, we have found that the current constraints on the lightest Higgs boson mass restrict very large value of the μ parameter. Conversely, the current limit from BR($B_s \to \mu^+\mu^-$) [19] also puts a severe constraint on the $\tan\beta$. As a result of these two combined effects, we have found that the contribution of the staus in the $h_1 \to \gamma\gamma$ process is highly limited as shown by the blue/dark-grey points in Fig. 4.

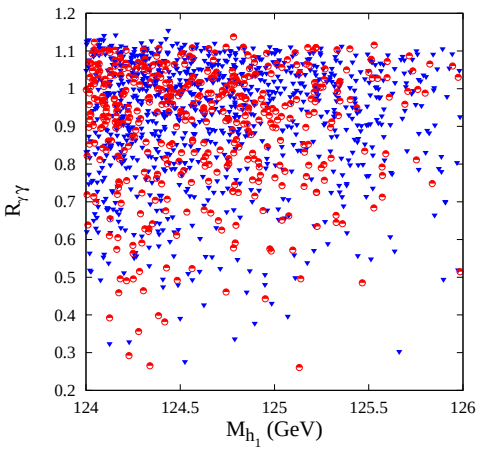

Figure 5: $R_{\gamma\gamma}$ vs M_{h_1} for all points considered in the CPV-MSSM (blue/dark grey) and CPC-MSSM (red/medium grey).

4 Results for the LHC Higgs signals

The main production channel in the context of the present LHC results is Gluon-Gluon Fusion (GGF), which at lowest order occurs at one-loop level, with the Higgs state decaying into $\gamma\gamma$ or $ZZ^* \to 4\mathrm{l}$[1]. The decay of the Higgs boson via the di-photon channel is also a one-loop process, unlike the ZZ^* one, which is tree level. The decay loops contain SUSY particles like stop, sbottom, stau, charginos and charged Higgs bosons in addition to the SM particles (top, bottom and charged gauge bosons), whereas the production loops only contain coloured particles (top, bottom, stop and sbottom). Furthermore, as we have assumed the Narrow Width Approximation (NWA) throughout[2] and neglected higher order QCD corrections at production level[3], we can compute the Higgs boson event ratios as follows:

$$R_{XX} \;=\; \frac{\Gamma(h_1 \to gg)^{\mathrm{CPV-MSSM}}}{\Gamma(h \to gg)^{\mathrm{SM}}} \times \frac{\mathrm{BR}(h_1 \to XX)^{\mathrm{CPV-MSSM}}}{\mathrm{BR}(h \to XX)^{\mathrm{SM}}} \tag{6}$$

where, $XX = \gamma\gamma$ or ZZ^* and h_1 is the lightest Higgs boson of the CPV-MSSM, while in the SM case it is marked as h. We proceeded similarly for the CPC-MSSM, wherein h_1 is meant to be replaced by the lightest CP-even Higgs boson.

[1] We neglect here consideration of the $\tau^+\tau^-$, $b\bar{b}$ and $WW^* \to 2\mathrm{l}2\nu$ modes from GGF, as experimental errors here are still very large.

[2] This is justified by the fact that in all models considered (SM, CPC-MSSM and CPV-MSSM) one has that the Higgs width is always several orders of magnitude smaller than the Higgs mass.

[3] Which would induce a different finite term inside the K-factor in the SM with respect to the CPV-MSSM (and CPC-MSSM as well).

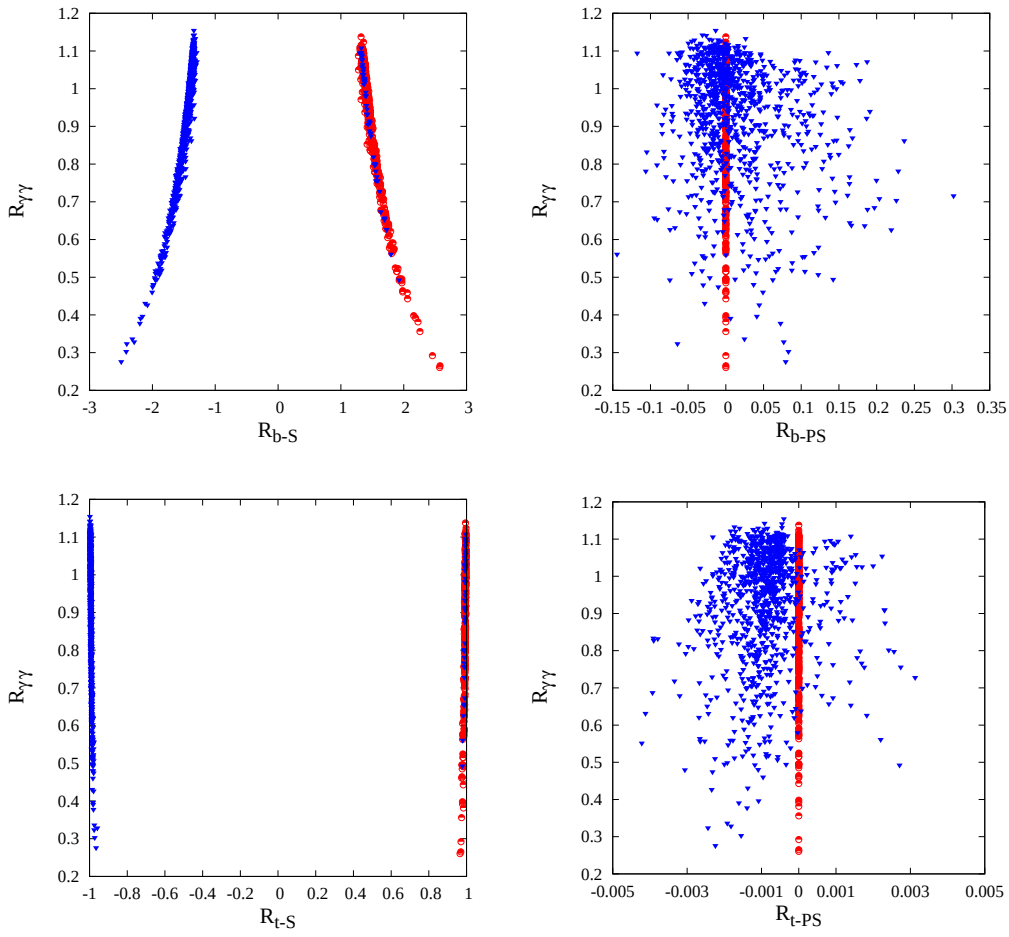

Figure 6: Variation of $R_{\gamma\gamma}$ with the scalar and pseudo-scalar part of the ratio of the bottom ((a) & (b)) and top ((c) & (d)) quark Yukawa couplings defined in eq. (7) in the CPV-MSSM (blue/dark grey) and CPC-MSSM (red/medium grey).

In Fig. 5 we have shown the variation of $R_{\gamma\gamma}$ with the Higgs mass M_{h_1}. We again have focused our attention onto the region where the Higgs mass varies between 124 and 126 GeV. It is clear from this plot that slightly larger values of $R_{\gamma\gamma}$ can be obtained within the CPV-MSSM with respect to the CPC-MSSM. Notice that we have followed the following color scheme while plotting all the relevant figures throughout the remainder of the analysis part: blue triangles (dark grey) correspond to CPV-MSSM and red circles (medium grey) to CPC-MSSM.

Notice that CPV effects enter eq. (6) through higher order corrections in the definition of the

physical h_1 mass as well as through lowest order terms via the $h_1\tilde{f}\tilde{f}^*$ couplings (here, $\tilde{f}$ refers to any possible sfermion). However, as emphasized in Refs. [21, 22], the most significant CPV effects are induced by the latter, since the former is responsible for mass shifts between models which are within current experimental uncertainties in the determination of the resonant Higgs mass.

In order to appreciate such effects in our analysis, we find it convenient to study the ratio of the bottom/top Yukawa coupling for the h_1 state of the CPV-MSSM relative to SM values for the h boson, which can be written as ($q = b, t$):

$$\frac{y_q^{\rm CPV-MSSM}}{y_q^{\rm SM}} = R_{q-S} + i\gamma_5 R_{q-PS} \tag{7}$$

(Again, a similar expression holds for the CPC-MSSM.) Thus, R_{q-S} denotes the scalar part of the coupling, while R_{q-PS} denotes the pseudo-scalar part. The full expressions for these terms can be found in the CPSuperH manual [18]. When $R_{\gamma\gamma}$ is plotted as a function of the b-quark couplings, R_{b-S} and R_{b-PS}, as shown in Fig. 6(a,b), one finds that there are solutions to the LHC Higgs data with both positive and negative couplings R_{b-S}, which is typical of the CPV-MSSM, unlike the case of the CPC-MSSM, which only allows for positive values. A similar behaviour is obtained for the dependence on the t-quark couplings, as shown in Fig. 6(c,d). Further, if one recalls that the coupling of top quark to the h_1 Higgs boson is inversely proportional to sinβ (relative to the SM case) and that we have varied tanβ from 1 to 20 (which implies sin$\beta \sim 1$), it is not surprising to see that R_{t-S} lies around unity. Needless to say, by definition, R_{b-PS} and R_{t-PS} are zero in the CPC-MSSM, whereas this is not so in the CPV-MSSM, where, however, their absolute values are much smaller than those for R_{b-S} and R_{t-S}, respectively.

We have studied the correlations between $R_{\gamma\gamma}$ and R_{ZZ} emerging from the GGF channel, as defined in eq. (6). From Fig. 7(a), we can conclude that values of $R_{\gamma\gamma}$ above 1 correspond to values of R_{ZZ} above 1.2. Though these values are somewhat in contradiction with (some) LHC data, which privilege $R_{\gamma\gamma}$ values larger than R_{ZZ}, at least according to the last updates from the CMS collaboration [23–25], our results are still consistent with data when one includes statistical fluctuations around the experimental best-fit value. According to the CMS collaboration the signal strength for the $\gamma\gamma$ channel is (1.56 ± 0.43) while for the ZZ channel is $(0.8^{+0.35}_{-0.28})$ [23–25]. To illustrate this, we have plotted our results against the latter along with the corresponding experimental 1σ and 2σ error bands in Fig. 7(b). Herein, the star marks the best-fit value (0.8, 1.56) of R_{ZZ} and $R_{\gamma\gamma}$ respectively from the CMS collaboration, and the yellow and green patches correspond to the 2σ and 1σ band drawn around it, respectively. In essence, the CPV-MSSM results are consistent with the CMS data within the 2σ error band (and so are the CPC-MSSM ones).

As we have already discussed, the main SM Higgs boson production mechanism at the LHC is GGF. However, the detection of the $h \to b\bar{b}$ and $h \to \tau^+\tau^-$ decays (and, similarly for the CPV-

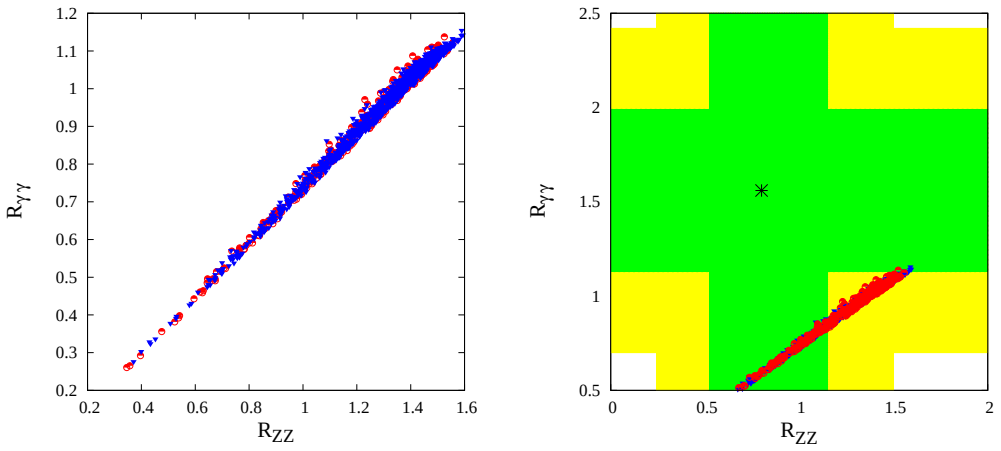

Figure 7: Correlation between $R_{\gamma\gamma}$ and R_{ZZ} when the Higgs boson is produced via GGF. Panel (a) shows our analysis while panel (b) the comparison with the recent LHC data along with the error bands around the experimental best-fit value. Blue(dark grey) and red(medium grey) colour coding as in Fig. 5. However, we have here plotted red before blue(blue before red) in the left(right) plot, in order to better appreciate the spreads of the CPV-MSSM and CPC-MSSM points.

MSSM and CPC-MSSM) are considered nearly impossible when the Higgs boson is produced this way, since it is expected to be overshadowed by di-jet events from QCD interactions. However, when the Higgs boson is produced in association with a vector boson (W/Z), also known as Higgs-strahlung (HS), with the gauge bosons decaying leptonically, it is relatively easy to tag the two b-jets to reconstruct the Higgs mass and both ATLAS and CMS have some sensitivity in this channel [26,27]. Hence, we have considered here this Higgs production channels when searching for Higgs boson signals decaying into pairs of bottom quarks or tau leptons. In this case, the definition of the corresponding event ratios will be modified to:

$$R_{YY} \;=\; \frac{\Gamma(h_1 \to VV)^{\rm CPV-MSSM}}{\Gamma(h \to VV)^{\rm SM}} \frac{{\rm BR}(h_1 \to YY)^{\rm CPV-MSSM}}{{\rm BR}(h \to YY)^{\rm SM}}, \tag{8}$$

where $YY = b\bar{b},\ \tau^+\tau^-$ (and $V = W/Z$ as well, since sensitivity to these decay modes also exists for the HS production mode[4]).

In Fig. 8 we have displayed the scatter plots in (a) $R_{\gamma\gamma} - R_{bb}$ plane and (b) $R_{\gamma\gamma} - R_{\tau\tau}$ plane in the CPV-MSSM (blue/dark grey points) and CPC-MSSM (red/light grey points), respectively.

[4]Notice that the ratio relative to the SM of the h_1 couplings to W and Z bosons is the same in the CPV-MSSM and CPC-MSSM.

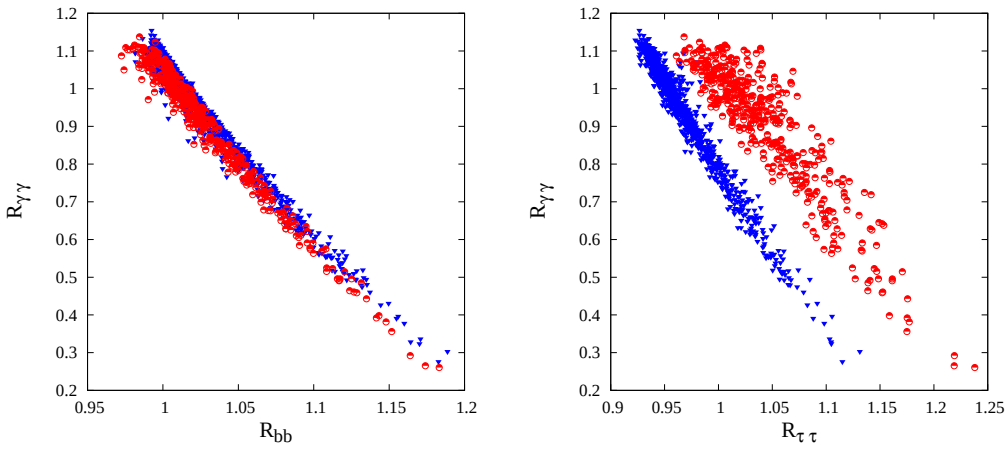

Figure 8: Correlation between (a) $R_{b\bar{b}}$ and $R_{\gamma\gamma}$ and (b) between $R_{\tau\tau}$ and $R_{\gamma\gamma}$ in the CPV-MSSM (blue/dark grey) and CPC-MSSM (red/light grey). Here, the Higgs boson is produced in association with a gauge boson W/Z.

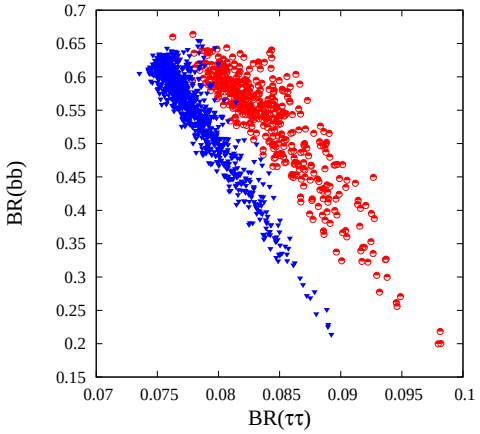

Figure 9: Correlation between the BRs of the lightest Higgs boson of the CPV-MSSM (blue/dark grey) and CPC-MSSM (red/light grey) into pairs of b's and τ's. Again, we assume here Higgs boson production via HS.

First, we have checked that the change in $\Gamma(h, h_1 \to VV)$ in the presence of CP-violating phases with respect to the SM is negligible for all the allowed points. Hence, from eq. (8), it is clear

that R_{YY} mainly depends on BR$(h, h_1 \to YY)$. To understand this, in Fig. 9, we have shown the correlation between the BRs of the Higgs boson into pairs of b's and τ's. In the case of the CPV-MSSM, the Higgs boson partial decay width into a pair of τ's is suppressed compared to the CPC-MSSM. Hence, the shift of the CPV-MSSM points towards lower values of $R_{\tau\tau}$ is the artifact of the suppression in BR$(h_1 \to \tau\tau)$. Since the BR$(h_1 \to b\bar{b})$ does not change by a significant amount in the CPV-MSSM relative to the CPC-MSSM, we cannot expect any noticeable difference in this particular decay mode. Thus, looking at this two particular decay profiles, one can come to two conclusions. On the one hand, present results from the LHC are in good agreement with both the CPV-MSSM and CPC-MSSM predictions. On the other hand, a close scrutiny of the BR$(h_1 \to b\bar{b})$ and BR$(h_1 \to \tau^+\tau^-)$ will enable one to distinguish between the two SUSY hypotheses.

5 Conclusions

In this paper, we have studied the possibility to have a SM-like Higgs boson with mass around 125 GeV in the CPV-MSSM in compliance with recent LHC data. Furthermore, we have checked that there exists agreement between the CPV-MSSM and said data while examining the event rates in the Higgs boson detection channels to which ATLAS and CMS have established sensitivity, particularly in the case of the $gg \to h_1 \to \gamma\gamma$ mode. In both instances, we have highlighted the role of the complex phases, by comparing the CPV-MSSM to the CPC-MSSM, in presence of known experimental constraints, such as those extracted from flavor-violating processes, CPV observables and Electric Dipole Moments (EDMs). Finally, we have shown how studying correlations between the $b\bar{b}$ and $\tau^+\tau^-$ detection channels may enable one to distinguish the CPV-MSSM and CPC-MSSM.

Acknowledgments

A.C. would like to acknowledge the hospitality provided by IIT Guwahati where part of this work was done. J.L.D.-C. acknowledges support from VIEP-BUAP and CONACYT-SNI (Mexico). The work of S.M. is supported in part through the NExT Institute. The work of P.P. and B.D. is supported by a SERC, DST (India) project, SR/S2/HEP-41/2009. A.C. would like to thank Dr. Debottam Das and Dr. Biplob Bhattacherjee for useful discussions.

References

[1] ATLAS Collaboration, Phys. Lett. B **716**, 1 (2012).

[2] CMS Collaboration, Phys. Lett. B **716**, 30 (2012).

[3] For reviews on Supersymmetry, see, J. Wess and J. Bagger, *Supersymmetry and Supergravity*, 2nd ed., (Princeton University Press, Princeton, 1991); M. Drees, P. Roy and R. M. Godbole, *Theory and Phenomenology of Sparticles*, (World Scientific, Singapore, 2005); H. E. Haber and G. Kane,Phys. Rep. **117**, 75 (1985); H. P. Nilles, Phys. Rep. **110**, 1 (1984).

[4] S. P. Martin, arXiv:9709356 [hep-ph].

[5] A. Djouadi, Phys. Rept. **457**, 1 (2008).

[6] A. Djouadi, Phys. Rept. **459**, 1 (2008).

[7] A. Arbey, M. Battaglia, A. Djouadi and F. Mahmoudi, arXiv:1211.4004 [hep-ph]; P. Bechtle, S. Heinemeyer, O. Stal, T. Stefaniak, G. Weiglein and L. Zeune, arXiv:1211.1955 [hep-ph]; K. Schmidt-Hoberg, F. Staub and M. W. Winkler, JHEP **1301**, 124 (2013); Z. Heng, arXiv:1210.3751 [hep-ph]; M. Drees, Phys. Rev. D **86**, 115018 (2012) A. Arbey, M. Battaglia, A. Djouadi and F. Mahmoudi, JHEP **1209** (2012) 107 K. Schmidt-Hoberg and F. Staub, JHEP **1210**, 195 (2012); M. Carena, I. Low and C. E. M. Wagner, JHEP **1208** (2012) 060 M. Carena, S. Gori, N. R. Shah and C. E. M. Wagner, JHEP **1203** (2012) 014 S. Heinemeyer, O. Stal and G. Weiglein, Phys. Lett. B **710**, 201 (2012); A. Arbey *et al.*, Phys. Lett. B **708**, 162 (2012); L. J. Hall, D. Pinner and J. T. Ruderman, JHEP **1204**, 131 (2012); P. Draper *et al.*, N. Chen and H. -J. He, JHEP **1204**, 062 (2012); G. Guo, B. Ren and X. G. He, arXiv:1112.3188 [hep-ph]; X. G. He, B. Ren and J. Tandean, arXiv:1112.6364 [hep-ph]; A. Djouadi, *et al.*, Phys. Lett. B **709**, 65 (2012); K. Cheung and T. -C. Yuan, Phys. Rev. Lett. **108**, 141602 (2012); B. Batell, S. Gori and L. -T. Wang, arXiv:1112.5180 [hep-ph]; T. Li, J. A. Maxin, D. V. Nanopoulos and J. W. Walker, Phys. Lett. B **710**, 207 (2012).

[8] H. Baer, V. Barger, A. Mustafayev, Phys. Rev. D **85**, 075010 (2012); J. F. Gunion, Y. Jiang and S. Kraml, Phys. Lett. B **710**, 454 (2012); L. Aparicio, D. G. Cerdeno and L. E. Ibanez, JHEP **1204**, 126 (2012); J. Ellis and K. A. Olive, arXiv:1202.3262 [hep-ph]; H. Baer, V. Barger and A. Mustafayev, arXiv:1202.4038 [hep-ph]; N. Desai, B. Mukhopadhyaya and S. Niyogi, arXiv:1202.5190 [hep-ph]. J. Cao, Z. Heng, D. Li and J. M. Yang, Phys. Lett. B **710**, 665 (2012).

[9] S. F. King, M. Muhlleitner, R. Nevzorov and K. Walz, arXiv:1211.5074 [hep-ph]; J. F. Gunion, Y. Jiang and S. Kraml, Phys. Rev. D **86** (2012) 071702 G. Belanger, U. Ellwanger, J. F. Gunion, Y. Jiang, S. Kraml and J. H. Schwarz, arXiv:1210.1976 [hep-ph]; J. F. Gunion, Y. Jiang and S. Kraml, Phys. Lett. B **710**, 454 (2012); U. Ellwanger and C. Hugonie, Adv. High Energy Phys. **2012**, 625389 (2012); U. Ellwanger, JHEP **1203**, 044 (2012); J. Cao, Z. Heng,

J. M. Yang, Y. Zhang and J. Zhu, JHEP **1203**, 086 (2012); Z. Kang, J. Li and T. Li, JHEP **1211**, 024 (2012).

[10] A. Elsayed, S. Khalil and S. Moretti, Phys. Lett. B **715**, 208 (2012); L. Basso and F. Staub, arXiv:1210.7946 [hep-ph].

[11] O. Stal and G. Weiglein, arXiv:1108.0595 [hep-ph]; K.E. Williams, H. Rzehak and G. Weiglein, Eur. Phys. J. **C71**, 1669 (2011); F. Deppisch and O. Kittel, JHEP **0909**, 110 (2009) [Erratum-*ibid.* **1003**, 091 (2010)]; R.M. Godbole, S. Kraml, S.D. Rindani and R.K. Singh, Phys. Rev. **D74**, 095006 (2006); S.Y. Choi, M. Drees, J.S. Lee and J. Song, Eur. Phys. J. **C25**, 307 (2002); A. Arhrib, D.K. Ghosh and O.C.W. Kong, Phys. Lett. **B537**, 217 (2002); A.G. Akeroyd and A. Arhrib, Phys. Rev. **D64**, 095018 (2001); S.-Y. Choi, K. Hagiwara and J.S. Lee, Phys. Rev. **D64**, 032004 (2001), Phys. Lett. **B529**, 212 (2002); D. K. Ghosh, R. Godbole, and D. Roy, Phys. Lett. B **628**, 131 (2005); D. K. Ghosh, S. Moretti, Eur. Phys. J. **C42**, 341 (2005); B. Bhattacherjee, A. Chakraborty, D. Kumar Ghosh and S. Raychaudhuri, Phys. Rev. D **86**, 075012 (2012).

[12] J. R. Ellis, J. S. Lee and A. Pilaftsis, Phys. Rev. D **72**, 095006 (2005); M. S. Carena, J. R. Ellis, A. Pilaftsis and C. E. M. Wagner, Phys. Lett. B **495**, 155 (2000).

[13] H. Georgi, A. Pais,Phys. Rev. D **10** (1974) 1246; N. Maekawa, Phys. Lett. B **282**, 387 (1992); A. Pilaftsis, Phys. Lett. B **435**, 88 (1998).

[14] O. C.W. Kong, F. L. Lin, Phys. Lett. B **418**, 217 (1998); N. Haba, Phys. Lett. B **398**, 305 (1997); A. Pomarol, Phys. Lett. B **287**, 331 (1992).

[15] For a review of MSSM Higgs phenomenology see: S. Y. Choi, J. Kalinowski, Y. Liao and P. M. Zerwas, Eur. Phys. J. C **40** (2005) 555; J. R. Ellis, J. S. Lee and A. Pilaftsis, Phys. Rev. D **70** (2004) 075010; M. S. Carena, J. R. Ellis, A. Pilaftsis and C. E. M. Wagner, Nucl. Phys. B **625** (2002) 345; M. Carena *et al.*, "Report of the Tevatron Higgs working group," arXiv:hep-ph/0010338.; S.Y. Choi, M. Drees and J.S. Lee, Phys. Lett. **B481**, 57 (2000); G.L. Kane and L.-T. Wang, Phys. Lett. **B488**, 383 (2000). A. Pilaftsis and C.E.M. Wagner, Nucl. Phys. **B553**, 3 (1999); D.A. Demir, Phys. Rev. D **D60**, 055006 (1999); A. Pilaftsis, Phys. Rev. **D58**, 096010 (1998) and Phys. Lett. **B435**, 88 (1998); M. S. Carena, M. Quiros and C. E. M. Wagner, Nucl. Phys. B **461**, 407 (1996); M. S. Carena, J. R. Espinosa, M. Quiros and C. E. M. Wagner, Phys. Lett. B **355**, 209 (1995).

[16] A. Pilaftsis and C. E. M. Wagner, Nucl. Phys. B **553**, 3 (1999).

[17] M. Carena, J.R. Ellis, A. Pilaftsis and C.E.M. Wagner, Phys. Lett. **B495**, 155, (2000) and Nucl. Phys. **B586**, 92 (2000).

[18] J. S. Lee, M. Carena, J. Ellis, A. Pilaftsis and C. E. M. Wagner, arXiv:1208.2212 [hep-ph], Comput. Phys. Commun. **180**, 312 (2009); J. S. Lee, A. Pilaftsis, M. S. Carena, S. Y. Choi, M. Drees, J. R. Ellis and C. E. M. Wagner, Comput. Phys. Commun. **156**, 283 (2004).

[19] LHCb Collaboration, CERN-PH-EP-2012-335, LHCB-PAPER-2012-043, arXiv:1211.2674.

[20] M. Carena, S. Gori, N. R. Shah, C. E. M. Wagner and L. -T. Wang, JHEP **1207**, 175 (2012).

[21] A. Dedes and S. Moretti, Nucl. Phys. B **576**, 29 (2000) and Phys. Rev. Lett. **84**, 22 (2000).

[22] S. Hesselbach, S. Moretti, S. Munir and P. Poulose, J. Phys. Conf. Ser. **335**, 012020 (2011); AIP Conf. Proc. **1200**, 498 (2010); Phys. Rev. D **82**, 074004 (2010); [arXiv:0710.4923 [hep-ph]]; J. Phys. Conf. Ser. **110**, 072017 (2008) and Eur. Phys. J. C **54**, 129 (2008); S. Moretti, S. Munir and P. Poulose, Phys. Lett. B **649**, 206 (2007).

[23] CMS Collaboration, CMS PAS HIG-12-020.

[24] CMS Collaboration, CMS PAS HIG-12-042.

[25] CMS Collaboration, CMS PAS HIG-12-041.

[26] CMS Collaboration, CMS PAS HIG-12-044.

[27] CMS Collaboration, CMS PAS HIG-12-043.